# Supporting Information

## Xiong et al. 10.1073/pnas.1419714112

### SI Materials and Methods

**Animals.** Lrp4$^{mitt}$ mice, which were generated by using *N*-ethyl-*N*-nitrosourea (ENU) (1), were obtained from L. A. Niswander (Howard Hughes Medical Institute, University of Colorado). They were crossed with human skeletal α-actin (HSA) promoter-driven Cre (HSA–Cre) transgenic mice to generate muscle-rescued Lrp4-null allele (mr-Lrp4$^{mitt}$). Generation of Lrp4-floxed mice, crossing, and genotyping Lrp4$^{loxP}$ mice, in which the exon 1 of the Lrp4 gene was flanked by loxP sites, were described previously (2). The floxed Lrp4 (Lrp4$^{f/f}$) mice were crossed with osteocalcin (Ocn)–Cre and lysozymeM (LysM)–Cre transgenic mice to generate OB- or OC-selective conditional knockout (CKO) mutant mice, Lrp4$^{Ocn}$-cko and Lrp4$^{LysM}$-cko. The Ocn–Cre mice were kindly provided by Tom Clemens (Johns Hopkins Medical School). The LysM–Cre mice were purchased from The Jackson Laboratory (donated by Irmgard Foerster, University of Duesseldorf). The mutant mice were back-crossed into C57BL/5J mice. Mice were housed in a room with a 12 h light/dark cycle with ad libitum access to water and standard rodent chow diet (Harlan Tekled S-2335). Control littermates were processed in parallel for each experiment.

**Microcomputed Tomography.** The microcomputed tomography (μCT) imaging analysis was carried out as described previously (3, 4). In brief, microarchitecture of the distal trabecular bone and midshaft cortical bone of the femur were measured by Scanco μCT 40 (Scanco Medical AG, Brüttisellen, Switzerland). Bones were placed vertically in 12-mm-diameter scanning holders and scanned at the following settings: 12-μm resolution, 55-kVp energy, 145-μA intensity, and an integration time of 200 ms.

**Bone Histomorphometric Analysis.** Bone histomorphometric analyses were carried out as previously described (3, 4). Briefly, mouse tibia and femurs were fixed overnight in 10% (vol/vol) buffered formalin, decalcified in 100 g/L EDTA, embedded in paraffin, sectioned, and subjected for H & E, Goldner Trichrome stain, and TRAP-staining analyses, which were counterstained by fast green. Bone histomorphometric perimeters were determined by measuring the areas situated at least 0.5 mm from the growth plate, excluding the primary spongiosa and trabeculae connected to the cortical bone.

**Measurements of Serum Levels of Osteocalcin, PYD, And Sclerostin.** Mouse serum samples were collected and subjected to ELISA analysis of osteocalcin and sclerostin and RIA analysis of PYD as described previously (3, 4). Mouse osteocalcin Elisa kit (Biomedical Technologies, Inc.), METRA Serum PYD RIA kit (QUIDEL Corporation), and mouse/rat *SOST* (sclerostin) Elisa kit (R&D Systems) were used. All of the samples were measured in duplicate, and values were subjected to statistical analysis.

For mouse serum levels of osteocalcin test, it was measured at a 1:5 dilutions of collected serum samples. Serum samples (25-μL diluted samples) were incubated at 4 °C overnight with 100 μL of biotin–mouse osteocalcin antibody. After three washes, 100 μL of HRP–Strep A were added and incubated in the dark at room temperature for 30 min. One hundred microliters of tetramethylbenzidine–Perox were then added after three washes to incubate for 15 min at room temperature. The reaction was stopped, and the OD was measured at 450 nm within 30 min of stopping reaction and then converted to osteocalcin concentrations using a standard curve.

For measurement of PYD, serum samples (25 μL) were incubated with PYD antibody solution (75 μL) overnight at 4 °C in the dark. After three washes, samples were incubated with enzyme conjugates for 60 min at room temperature and followed by three washes and incubation with substrate solution (150 μL) at room temperature for 40 min. The reaction was stopped, and the OD measured at 405 nm was converted to PYD concentrations using a standard curve.

For mouse serum levels of sclerostin, serum samples were measured at a twofold dilution and incubated for 3 h at room temperature with mouse/rat sclerostin antibody. After five washes, 100 μL conjugate were added and incubated for 1 h at room temperature and followed by five washes and incubation with 100 μL substrate solution for 30 min at room temperature in the dark. The reaction was stopped, and the OD was measured at 450 nm. Five hundred forty nanometers was used for wavelength correction and then converted to sclerostin concentrations using a standard curve.

**Dynamic Bone Histomorphometry to Measure the Rate of Bone Formation In Vivo.** Briefly, mice (2 wk old) were injected (intraperitoneally) with fluorochrome-labeled calcein green (10 mg/kg, Sigma–Aldrich) and then with Alizarin Red S (50 mg/kg, Sigma–Aldrich) (12 d interval). The mice were killed 2 d after the second injection. The left tibia and femurs were fixed in 70% (vol/vol) ethanol overnight, embedded in methyl methacrylate, and sectioned at 7–10 μm. Images were obtained using a 25× objective fluorescence microscope (laser scanning microscope 510; Carl Zeiss). The mineral apposition rate (MAR) in μm/d and bone formation rate (BFR) [BFR = MAR × MS (mineral surface) / BS (bone surface)] were calculated from fluorochrome double-labels at the periosteal and endocortical surfaces.

**Plasmids and Transient Transfection.** The *SOST* cDNA was cloned into pcDNA3.1 plasmid. Both DKK1 and agrin expression plasmids were generated by insert DKK1/agrin into pFlag–CMV1 downstream of a signal peptide. The Flag–Lrp4 and Flag–ecto-Lrp4 (Lrp4–ECD) plasmids were generated by insertions of the full-length Lrp4 and ecto-Lrp4 cDNA into the pFlag–CMV1 vector, which has an artificial signal peptide and a Flag epitope. The authenticity of all constructs was verified by DNA sequencing.

HEK293 cells were maintained in Dulbecco-modified Eagle medium supplemented with 10% FCS and 100 units/mL of penicillin G and streptomycin (Gibco). Calcium phosphate method was used for transfection of HEK293 cells. Forty-eight hours following transfection, cells were lysed in modified RIPA immunoprecipitation assay buffer (50 mM Tris·HCl, pH 7.4, 150 mM sodium chloride, 1% Nonidet P-40, 0.25% sodium deoxycholate, proteinase inhibitors). Lysates and medium were subjected to immunoblotting analyses.

**In Vitro OB Culture and Treatments with Lrp4 Ligands: Sclerostin, DKK1, Agrin, Wise, and Lrp4–ECD.** Whole bone marrow cells were isolated from long bones of 8-wk-old WT and Lrp4 mutant mice and plated on 100-mm tissue culture plates in DMEM containing 10% (vol/vol) FBS, 1% penicillin/streptomycin (P/S). After 7 d, passaging cells by trypsin digestion, $1 \times 10^4/cm^2$ were plated for osteogenesis differentiation in the presence of osteogenic medium [DMEM containing 10% (vol/vol) FBS, 1% P/S,10 mM β-glycerophosphate, and 50 μM L-ascorbic acid–2-phosphate]. Medium contained control (pcDNA3.1), sclerostin, Flag–DKK1, Flag–agrin, or mixed Lrp4–ECD was added to the differentiation medium (DM) (at a ratio of 1:1) at every medium change. Recombinant Wise protein (Abcam) was added to the DM at a

concentration of 100 ng/mL 7 d after incubation, ALP-staining (Sigma) and quantification analyses were performed.

**RNA Isolation and Real-Time PCR.** Total RNA was isolated from BMSCs by TRIzol extraction (Invitrogen). Quantitative PCR was performed with a Quantitect SYBR Green PCR Kit (Bio-Rad), according to the manufacturers's instructions, and with a Real-Time PCR System with analytical software (Opticon Monitor 3). The following primers were used: M-CSF, 5′-TTGGCTTGGGATGATTCTCAG-3′ and 5′-GCCCTGGGTCTGTCAGTCTC-3′; RANKL, 5′-ATCCCATCGGGTTCCCATAA-3′ and 5′-TCCGTTGCTTAACGTCATGTTAG-3′; OPG, 5′-GGCCTGATGTATGCCCTCAA-3′ and 5′-GTGCAGGAACCTCATGGTCTTC-3′; Wnt5a, 5′-CAACTGGCAGGACTTTCTCAA-3′ and 5′-CATCTCCGATGCCGGAACT-3′; SOST, 5′-AGCCTTCAGGAATGATGCCAC-3′ and 5′-CTTTGGCGTCATAGGGATGGT-3′; and DKK1, 5′-CTCATCAATTCCAACGCGATCA-3′ and 5′-GCCCTCATAGAGAACTCCCG-3′. β-actin primers (5′-AGGTCATCACTATTGGCAACGA-3′ and 5′-CATGGATGCCACAGGATTCC-3′) were used for normalization.

**Statistical Analysis.** All data were expressed as mean ± SD. The significance level was set at $P < 0.05$. Student $t$ test was used for statistical analysis.


1. Weatherbee SD, Anderson KV, Niswander LA (2006) LDL-receptor-related protein 4 is crucial for formation of the neuromuscular junction. *Development* 133(24): 4993–5000.
2. Wu H, et al. (2012) Distinct roles of muscle and motoneuron LRP4 in neuromuscular junction formation. *Neuron* 75(1):94–107.
3. Xia WF, et al. (2013) Vps35 loss promotes hyperresorptive osteoclastogenesis and osteoporosis via sustained RANKL signaling. *J Cell Biol* 200(6):821–837.
4. Xia WF, et al. (2013) Swedish mutant APP suppresses osteoblast differentiation and causes osteoporotic deficit, which are ameliorated by N-acetyl-L-cysteine. *J Bone Miner Res* 28(10):2122–2135.


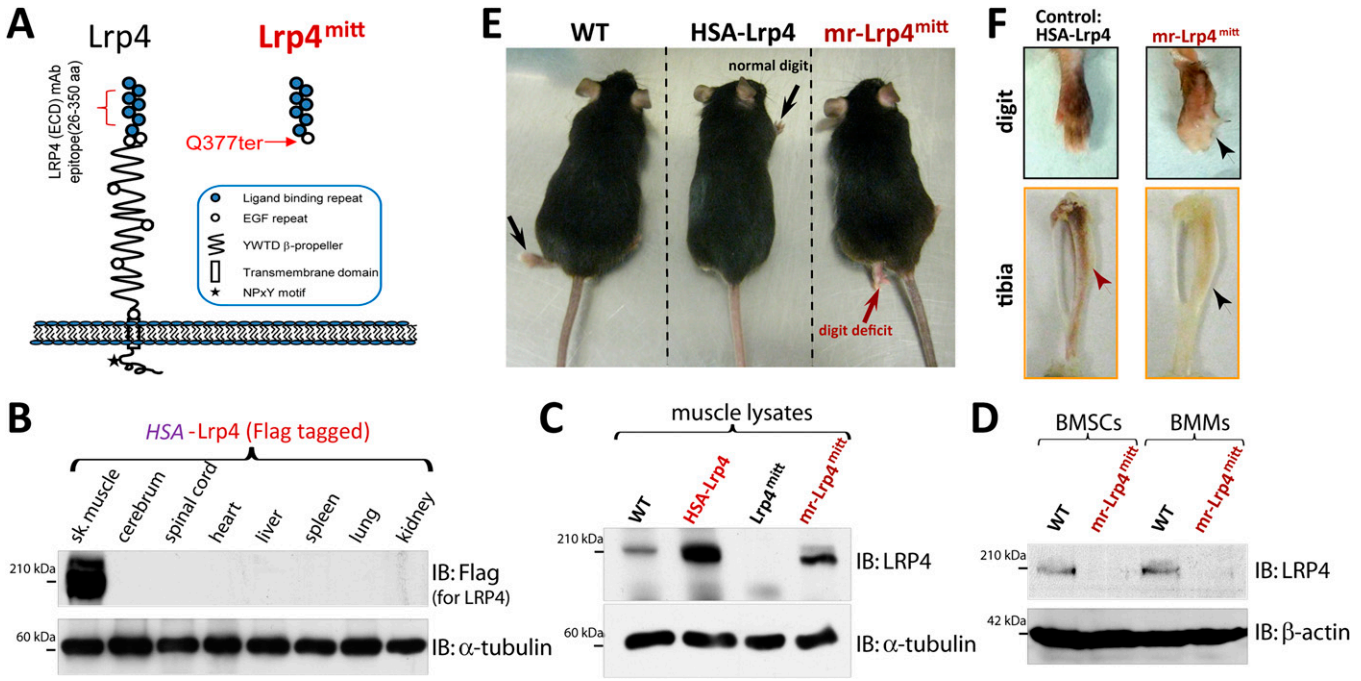


**Fig. S1.** Generation of muscle-rescued Lrp4-null (mr-Lrp4$^{mitt}$) mice. (*A*) Illustration of the LRP4 protein structure and the stop codon in Lrp4$^{mitt}$ mice. (*B*) Western blot analysis of Lrp4 (flag tagged) transgene expression in various tissue homogenates from HSA–Lrp4 mice. (*C* and *D*) Western blot analyses of Lrp4 expression in indicated tissue/cell lysates from control and mr-Lrp4$^{mitt}$ mice. (*E*) Images of control and mr-Lrp4$^{mitt}$ mice at the age of 3 mo old. (*F*) Digit defect and pale long bone in 3-mo-old mr-Lrp4$^{mitt}$ mice.

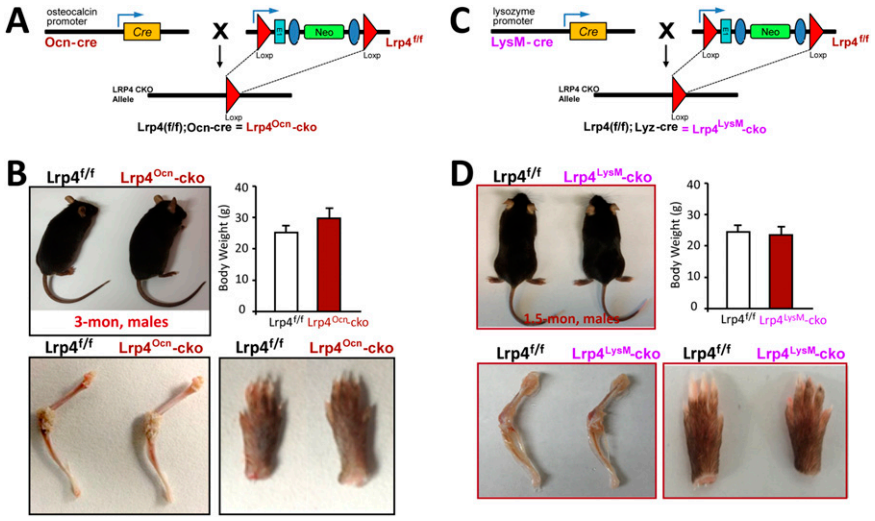


**Fig. S2.** Generation of OB- and OC-selective Lrp4 knockout mice. (*A* and *C*) Illustrations of breeding strategies for generation of Lrp4$^{Ocn}$-cko (*A*) and Lrp4$^{LysM}$-cko (*C*) mice. (*B* and *D*) Images, digits, and body weights of control vs. Lrp4$^{Ocn}$-cko (*B*) or vs. Lrp4$^{LysM}$-cko (*D*) mutant mice.

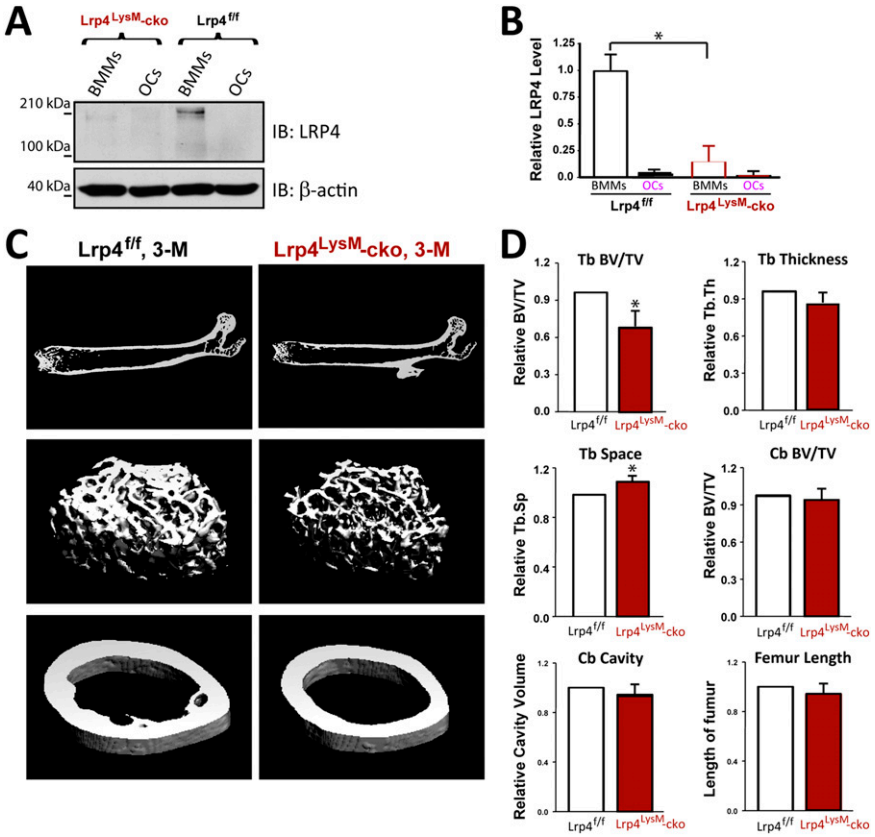


**Fig. S3.** Reduced trabecular, but not cortical, bone volumes in young adult Lrp4$^{LysM}$-cko mice. (*A* and *B*) Western blot analysis of LRP4 expression in BMSCs, OBs, BMMs, and OCs derived from 2-mo-old Lrp4$^{f/f}$ (control) and Lrp4$^{LysM}$-cko mice. Representative blots are shown in *A*. Quantification analysis (mean ± SEM, $n = 3$) is presented in *B*. (*C* and *D*) The μCT analysis of femurs from ~3-mo-old control (Lrp4$^{f/f}$) and Lrp4$^{LysM}$-cko littermates. Three different male mice of each genotype were examined blindly. Representative images are shown in *C*. Quantification analyses (mean ± SD, $n = 3$) are presented in *D*. *$P < 0.05$, significant difference from the control littermates.

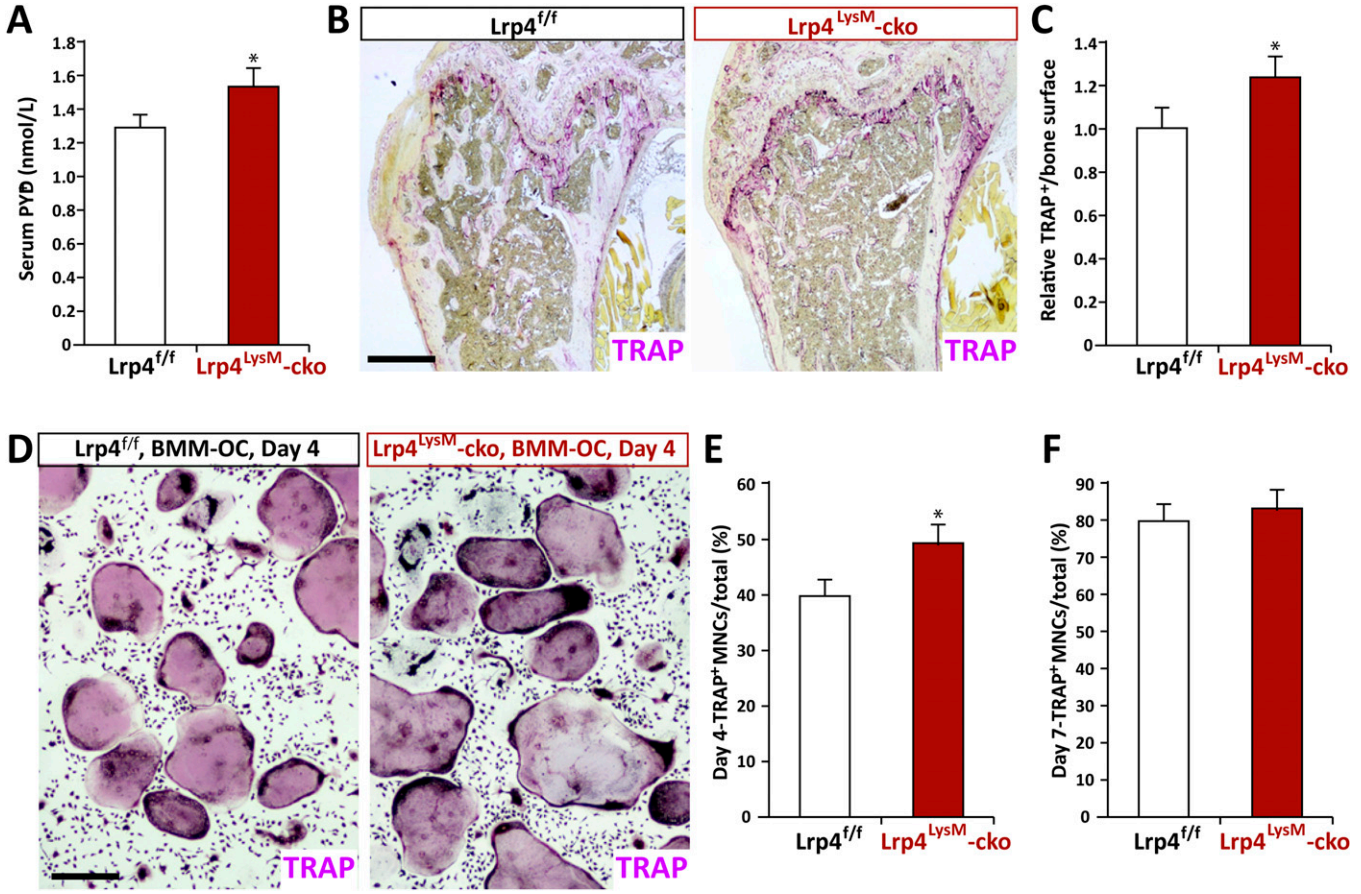


**Fig. S4.** Increased serum PYD and TRAP$^+$ OCs in Lrp4$^{LysM}$-cko mice. (*A*) Measurements of serum levels of PYD in ∼3-mo-old control and Lrp4$^{LysM}$-cko mice by RIA analyses. The values of mean ± SD from three different males per genotype are shown. *$P < 0.05$, significant difference from the control. (*B* and *C*) TRAP-staining analysis of femur sections from ∼3-mo-old control and Lrp4$^{LysM}$-cko littermates (three mice per age group per genotype, both males and females). Representative images are shown in *B*. (Scale bar, 100 μm.) The quantitative analysis of TRAP$^+$ cells per unit bone surface (BS) in trabecular bones is presented as values of mean ± SD from three different animals in *C*. *$P < 0.05$, significant difference from the control. (*D–F*) TRAP-staining analysis of cultured OCs derived from BMMs of 1.5-mo-old control and Lrp4$^{LysM}$-cko mice. Representative images of the cultures treated with RANKL for 4 d (day 4) are shown in *D*. (Scale bar, 150 μm.) The quantitative analyses of TRAP$^+$ multinuclei cells (MNCs) over total cells at days 4 and 7 of RANKL treatments are presented in *E* and *F*, respectively. The values of mean ± SD from three different cultures are shown. *$P < 0.05$, significant difference from the control.

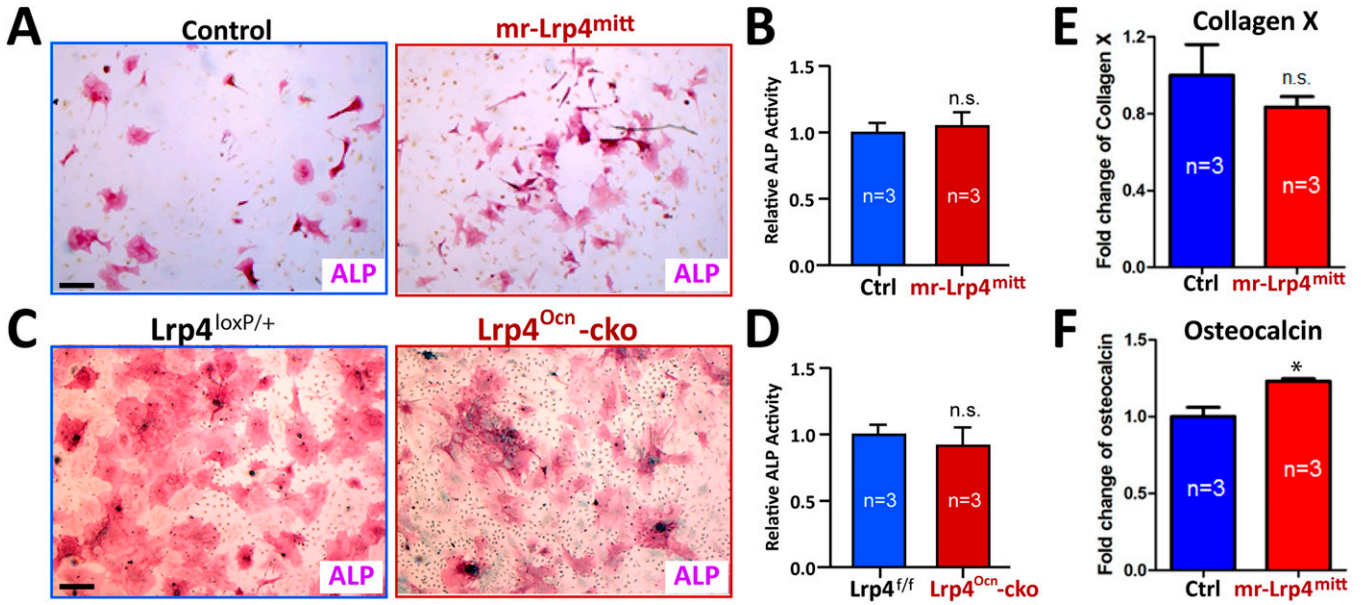


**Fig. S5.** Normal ALP activity, but increased osteocalcin expression, in Lrp4-deficient BMSCs. (*A–D*) Normal in vitro OB differentiation of BMSCs derived from control and indicated Lrp4 mutant mice (2 mo old). Representative images of ALP-staining analysis of OBs (day 14 OB culture of BMSCs isolated from 2-mo-old control and indicated Lrp4 mutant femur bone marrows) are shown in *A* and *C*. Quantitative analyses of the average ALP activities (mean ± SD from three different cultures) are presented in *B* and *D*. (Scale bars, 80 μm.) (*E* and *F*) Increased expression of osteocalcin (*F*), but not collagen X (*E*), in mr-Lrp4$^{mitt}$ BMSC culture by real-time PCR analysis. The values of mean ± SD from three different cultures are presented and normalized by their controls. *$P < 0.05$, significant difference.

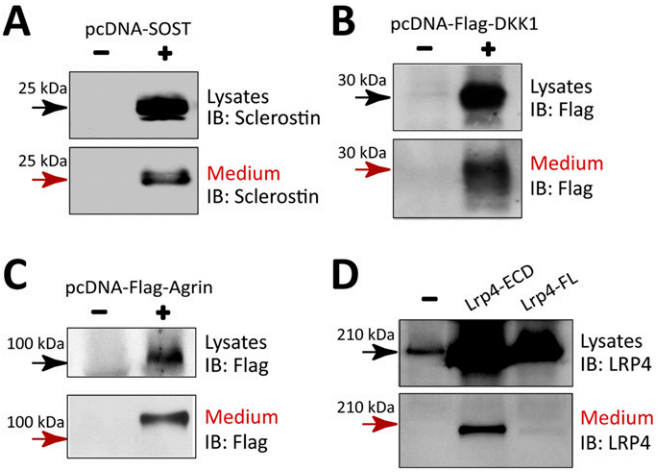


**Fig. S6.** Expression of sclerostin, DKK1, agrin, and Lrp4–ECD. HEK293 cells were transfected with indicated plasmids. The lysates and condition medium were subjected to Western blot analyses using indicated antibodies. Representative blots are shown in *A–D*.

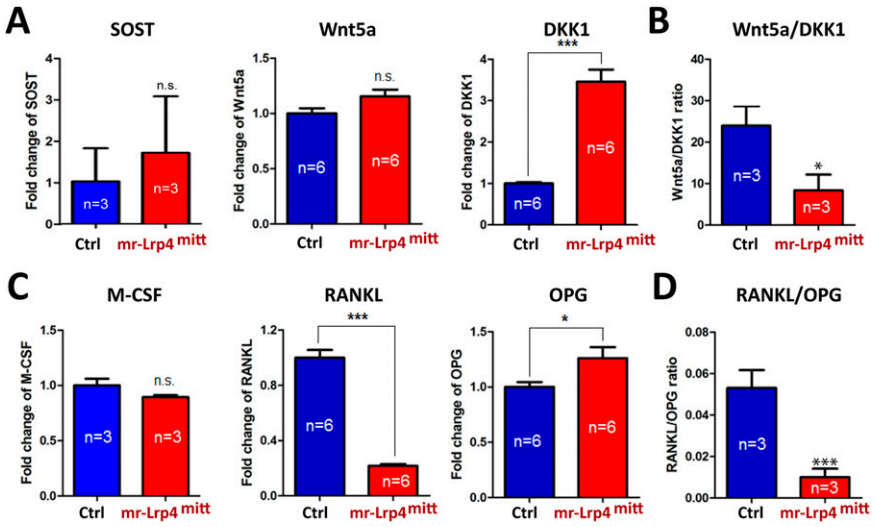


**Fig. S7.** Increased DKK1 and OPG, but decreased RANKL, in Lrp4-deficient BMSCs. (*A* and *C*) Real-time PCR analysis of the mRNA levels of Wnt5a, DKK1, M-CSF, RANKL, and OPG. The values are normalized to β-actin and controls (HSA–Lrp4 as control mice). Ratios of Wnt5a/DKK1 and RANKL/OPG are shown in *B* and *D*, respectively. Means ± SD values from three different experiments are presented. $*P < 0.05$, significant difference.